Eurographics Workshop on Visual Computing for Biology and Medicine (2018)
A. Puig Puig, T. Schultz, and A. Vilanova (Editors)

Annotated dendrograms for neurons from the larval fruit fly brain.

Martin Strauch[1] Volker Hartenstein[2] Ingrid V. Andrade[2] Albert Cardona[3] Dorit Merhof[1]

[1]Imaging and Computer Vision, RWTH Aachen University, Aachen, Germany
[2]Molecular, Cell and Developmental Biology, University of California, Los Angeles, USA
[3]Janelia Research Campus, Howard Hughes Medical Institute, Ashburn, USA

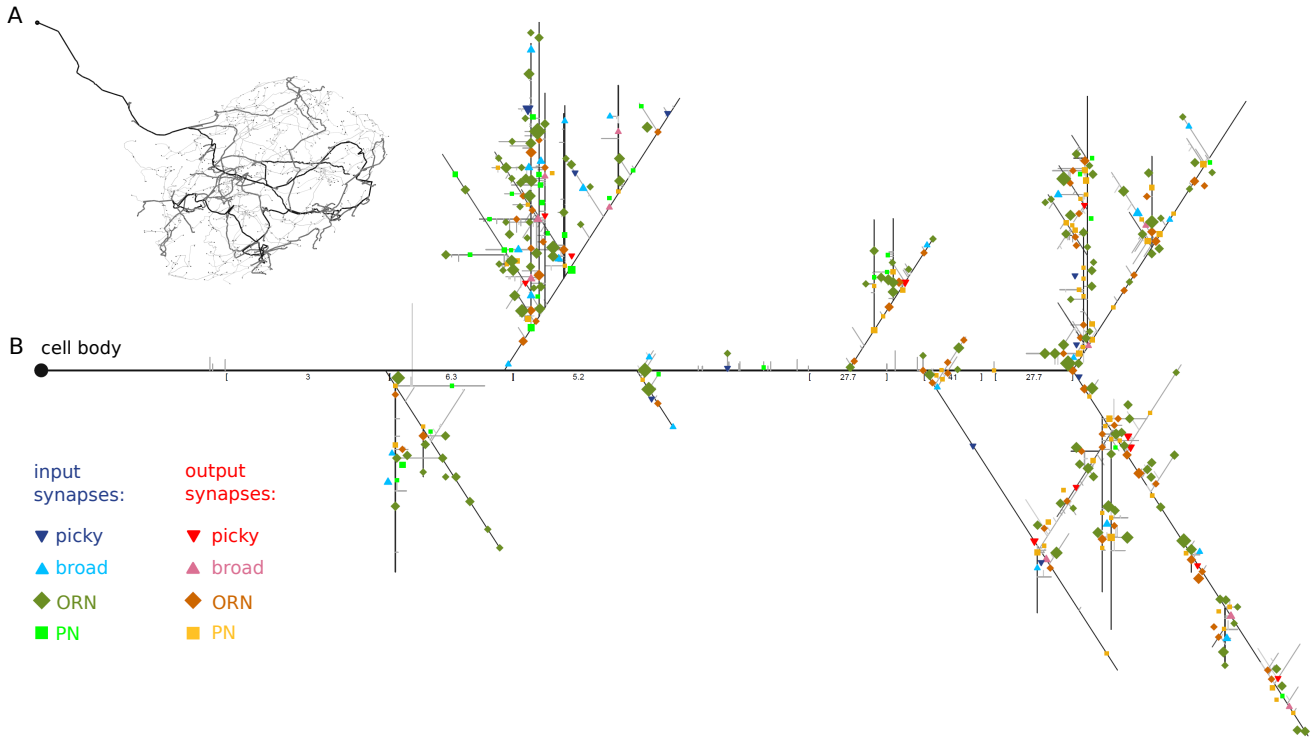

Figure 1: *(A) 3D reconstruction of a neuron from the larval fruit fly (broad interneuron from the antennal lobe).* ***(B)*** *The corresponding dendrogram with annotations that mark the sites of synaptic input from and output to four different neuron classes (see Section 2.1).*

Abstract

Recent advances in neuroscience have made it possible to reconstruct all neurons of an entire neural circuit in the larval fruit fly brain from serial electron microscopy image stacks. The reconstructed neurons are morphologically complex 3D graphs whose nodes are annotated with labels representing different types of synapses. Here, we propose a method to draw simplified, yet realistic 2D neuron sketches of insect neurons in order to help biologists formulate hypotheses on neural function at the microcircuit level. The sketches are dendrograms that capture a neuron's branching structure and that preserve branch lengths, providing realistic estimates for distances and signal travel times between synapses. To improve readability of the often densely clustered synapse annotations, synapses are automatically summarized in local clusters of synapses of the same type and arranged to minimize label overlap. We show that two major neuron classes of an olfactory circuit in the larval fruit fly brain can be discriminated visually based on the dendrograms. Unsupervised and supervised data analysis reveals that class discrimination can be performed using morphological features derived from the dendrograms.

CCS Concepts

• ***Human-centered computing*** → ***Visualization techniques; Scientific visualization;***

DOI: 10.2312/vcbm.20181229

1. Introduction

1.1. Motivation

Recently, morphological and connectivity information has become available for entire brain circuits. For example, all neurons of an olfactory [BKC*16] and a learning and memory center [ELLK*17] in the larval brain of the fruit fly *Drosophila melanogaster* have been reconstructed from serial electron microscopy stacks. A neuron reconstruction approach, as described in [SMGL*16], results in a 3D graph that captures a neuron's morphology. The graph is annotated with synapse labels, specifying at which position the neuron connects to which other neurons via synapses.

The advent of such brain reconstructions is accompanied by similar challenges as they were encountered when the first sequenced genomes became available. In the same way as we do not understand fruit fly genomics only because we have sequenced the fly's genome, brain reconstruction is only a prerequisite for understanding brain function. The wealth of data needs to be structured and analyzed, and the first step in this process is to visualize the morphology of single neurons and the locations of large numbers of synapses, the sites of neural connections, on the neurons.

In non-spiking local interneurons, which form more than half of the interneuron population in a typical insect ganglion, stimulus conduction is attenuated over time [SB79]. Hence, it is relevant where along the neuron a synapse is located, as a weak signal might vanish before it reaches a synapse at a remote location. In order to support the generation of hypotheses on neural function, a neuron visualization should thus preserve both the branching structure of a neuron and cable length distances between synapses.

1.2. The approach taken

Neuron visualization for data analysis, and in particular for figures in neurobiological papers, prompts the need for a compact, static neuron representation at a single level of detail. Given a reconstructed 3D neuron skeleton annotated with synapse labels, our goal is to provide a static 2D visualization that should be as realistic (preservation of branching structure and branch lengths) and clear (with minimal structural or synapse label overlap) as possible.

Our visualization approach is designed explicitly for insect neurons, where a single primary branch emanates from the cell body (Figure 1A), affording to draw a linearized version of the neuron, where the primary branch is represented by a straight line (Figure 1B). Due to complex neuron morphologies with overlapping and entangled side branches (Figure 1A), standard 2D projections are not suitable to resolve structural overlap. Instead, we regard a neuron as a tree rooted at the cell body, drawing a dendrogram that preserves the tree's branching structure (Section 2). In particular, we employ dendrograms with realistic branch lengths (Figure 1B) that preserve cable length distances between synapses. Large numbers of synapses can be displayed on the dendrograms through representing local synapse agglomerations by a single symbol and through arranging the symbols to minimize overlap.

For analytical purposes, we define features that describe the dendrograms' branches, showing that dendrograms of neurons from known neuron classes can be discriminated not only visually, but also by classification based on these features (Section 3).

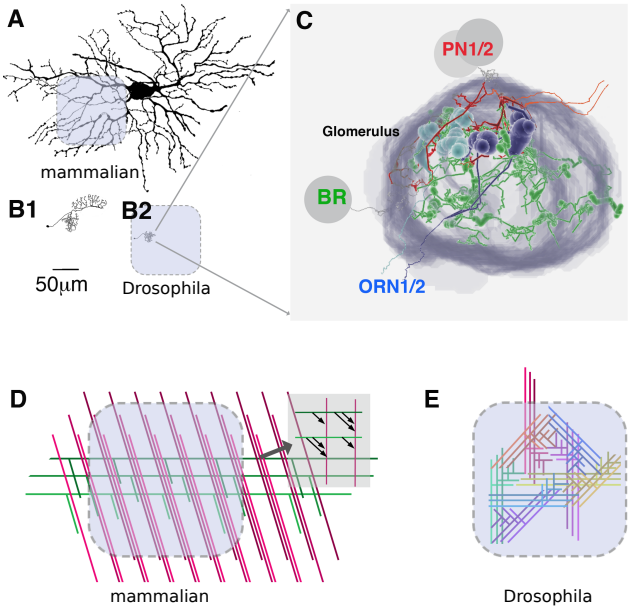

Figure 2: ***(A, B)*** *A typical mammalian neuron (**A**, retinal ganglion cell), a* Drosophila *neuron of the adult (**B1**; tangential neuron of the central complex) and of the larval fly brain (**B2**; antennal lobe interneuron) drawn to scale. Shaded areas indicate the approximate size of brain tissue volumes that can be processed with current technologies.* ***(C)*** *3D rendering of the* Drosophila *larval antennal lobe illustrating a broad interneuron (BR) and fragments of olfactory receptor (ORN) and projection neurons (PN) that form connections inside a structure called glomerulus.* ***(D, E)*** *Content that is accessible with current technology: For the mammalian brain* ***(D)****, the volume contains fragments of afferent fibers (red) forming synaptic input on fragments of efferent systems (green). Inset: synapses between afferent and efferent fibers. For* Drosophila*, entire brains with all neurons (arrays of branched lines), are included* ***(E)****.*

1.3. Neuron data

The first nervous system to be reconstructed at the single synapse level was that of *C. elegans*. Unlike the linear, unbranched neurons of *C. elegans*, the reconstructed *Drosophila* neurons considered here [BKC*16], are more complex: Even though they are smaller than mammalian neurons (Figure 2A,B), they resemble them in that they possess multiple specialized domains and highly branched neuron trees (Figure 2B1, C).

The current state of the art allows processing EM volumes of up to a few hundred μm. In the mammalian case, the circuits included in these volumes do mainly contain fragments of, rather than complete, neurons (Figure 2A, D), whereas for *Drosophila* we already have entire reconstructed circuits with full connectivity between complete neurons (Figure 2E).

In the typical mammalian case, several hundred axons originating from different cell types (whose somata and dendrites are outside the sectioned volume) intersect with systems of dendrites (whose somata and axons are also not included), and the analytical

goals are chiefly concerned with exploring connectivity patterns between terminal axons and dendrites: Does an axon connect to a dendrite multiple times? How are synapses clustered? (see e.g. Fig. 2C, inset in [ABS*14]).

In contrast, for our *Drosophila* EM data set (Section 2.1) all $\approx 10,000$ central neurons with all branches and synaptic connections are included in the volume measuring approximately $100 \times 100 \times 300\ \mu m$ (Figure 2B2, E). This presents us with great opportunities to analyze the full connectome of e.g. an olfactory circuit. The dendrogram visualizations are the basis for formulating hypotheses regarding the function of the circuit, which then can be tested experimentally.

1.4. Related work

1.4.1. Visualizing neuron morphology

Neurons are sometimes visualized by dendrograms in the form of abstract trees that preserve only the neuron's branching structure. For a survey on general tree visualization, see [Sch11].
More realistic neuron dendrograms also preserve branch lengths [CdFC99, Asc02]. Such dendrograms still resemble mathematical trees with two equal child branches at each branching point, while our dendrograms have a dominant primary branch with subordinate side branches, which is a more realistic depiction of insect neuron morphology.
The L-Neuron method generates (non-unique) morphologically realistic neuron trees based on parameters extracted from a homogeneous neuron population [AK00].

None of the above approaches considers synapse annotations and the difficulties associated with displaying large numbers of synapses on the dendrograms. Only our method and NeuroLines [ABS*14] create realistically looking dendrograms that preserve branch length, have a dominant primary branch and synapse annotations. NeuroLines visualizes mammalian data with incomplete neurons (see Section 1.3) and it also differs from our method with respect to the way it displays synapses. When nearby synapse labels overlap, NeuroLines summarizes all of these overlapping synapses by a cluster symbol. The content of the cluster can then be inspected by clicking on the symbol. In contrast, we summarize only nearby synapses *of the same type* with a symbol (scaled proportional to cluster size) and then carefully rearrange all synapse symbols to improve readability. NeuroLines is essentially an interactive software, where side branches can be unfolded and synapses be revealed upon the user's request. In contrast, our dendrograms show all synapses at once, i.e. they visualize neurons at a single level of detail and are also suitable for static displays, such as figures in neuroscience papers.

1.4.2. Visualizing neuron connectivity

Several approaches to visualizing neuron connectivity in the *Drosophila* brain are designed for optical microscopy volumes, where, different from our electron microscopy data, the exact synapse positions are not known. Instead, connectivity is estimated based on arborization overlap, which is a prerequisite for the existence of synapses. A tool for 3D visualization of the overlap of multiple arborizations has been presented in [SMB*17]. BrainGazer [BSG*09] is a software for 3D visualization of optical microscopy volumes from the *Drosophila* brain. One of the tools included in BrainGazer is neuroMap [SBS*13] that summarizes potential connectivity through wiring diagrams that are abstract visualizations: arborization nodes arranged in a circle are connected by edges whose transparency and grayscale values encode the amount of overlap. This is different from our realistic dendrograms with connections between individual, labelled and precisely positioned synapses.
Also neuron connectivity in a circuit of the mouse brain has been estimated based on structural overlap in light microscopic data sets [DEHO12]: An interactive tool allows displaying a selection of the estimated synapse positions, however not on dendrograms, but on reconstructed 3D neuron structures.

ConnectomeExplorer [BAK*13] is a software for interactive exploration of electron microscopy brain tissue volumes where neurons have been segmented and annotated, similar to our data. The software offers a 3D volume view, a query language and abstract neuron connectivity graphs.

1.4.3. Neuronal morphometry

The term *neuronal morphometry* refers to the extraction of morphological features from reconstructed neurons. A commonly used feature set for mammalian neurons can be computed with L-measure [SPA08], and such features have been used to characterize neurons or to discriminate neuron classes [CCJdFC16]. Here, we do not compute general feature sets for reconstructed neurons, but we rather define features to describe the information conveyed by our dendrogram visualizations.

The insect neurons used in this work project from an external cell body into a neural circuit where several side branches branch off from the neuron (Figure 1A). In contrast, mammalian neurons typically have a central cell body from which dendrites extend into several directions. A number of common neuronal morphometry approaches, such as the classical Sholl analysis [Sho53] and its recent implementations [FBO*14] and modifications [RMM*16] are explicitly targeted at such mammalian neurons, measuring the density of dendritic arborizations within a radius around the cell body.

In a wider sense, neuronal morphometry approaches also serve to perform structural similarity search in neuron databases, either through computing distances between feature vectors or by neuron registration and alignment [CMO*16]. Recently, methods relying on topological persistence have been proposed to represent an entire neuron tree by a signature or barcode [LWA*17, KDS*18], where similar neurons receive similar barcodes. Our dendrogram features could be used for similarity search, however they are not targeted at capturing overall neuron shape, but rather describe, for analytical purposes, properties of side branches.

2. Methods

2.1. Data set and neuron classes

The neuron reconstructions are based on an electron microscopy volume that has been manually segmented and annotated in a distributed effort, using the web interface CATMAID [SCHT09, SMGL*16] for data handling and visualization.

Current large-scale neuron reconstruction projects still rely on manual annotation and proofreading by experts [SMGL*16]. The resulting neuron skeletons (Figure 1A) consist of vertices denoting positions in the 3D space of the electron microscopy volume.

Here, we consider reconstructed neurons from the larval brain of the fruit fly. The data set from [BKC*16] provides neuron skeletons, including exact synapse locations, for all neurons from the antennal lobe (AL), an olfactory processing center. We focus on all members of four major neuron classes in the AL (s.a. Figure 2C): the *olfactory receptor neurons (ORNs)* that relay odor receptor signals to the AL, the *projection neurons (PNs)* that provide output from the AL to higher-order brain centers, and two classes of local interneurons that provide lateral connectivity, the GABAergic, presumably inhibitory, *broad interneurons* and the glutamatergic, presumably excitatory, *picky interneurons*. These connections form the substrate for multiple types of feed-back and feed-forward loops which are assumed to be important to shape the exact response of PNs to olfactory stimulation [BKC*16].

Broad interneurons meander among all glomeruli of the AL, contacting individual ORNs and PNs multiple times and locally forming input and output synapses with these elements. Picky interneurons have a more restricted arborization in local neighborhoods within the AL: They are polarized, receiving almost exclusively input on their proximal branches, and mixed input/output distally.

2.2. Graph representation

The dendrogram drawing procedure takes as input a connected, acyclic graph $G = (V, E)$, i.e. a tree, with vertices V that are connected by edges E. The graph is rooted at the neuron's cell body $v_0 \in V$. The vertices $v_i \in V$ denote equidistantly spaced points on the neuron for which coordinates in the 3D space of the electron microscopy stack are available. Vertices with two child vertices are branching points where a side branch branches off from the current branch. A subset of the vertices is annotated with synapse labels that contain information regarding the class of the connecting neuron and about whether the current neuron is the pre-synaptic partner (output synapse) or the post-synaptic partner (input synapse).

2.3. Dendrogram drawing

Visualization of neuron morphology and synapse positions is impaired by branches that overlap and form loops. For the sake of readability, we therefore wish to "linearize" the neuron, introducing a dominant primary branch that emanates from the cell body and forms side branches, connecting branching points by straight lines and deflecting side branches at stereotyped angles to avoid branch overlap (Table 1).

Starting at the root, we traverse the graph G, continuing at each branching point the branch with the higher weight $w(\text{branch})$ as a straight line: From this primary branch, the side branches with lower weights are deflected, "major side branches" at a 45° angle and "minor side branches" at a 90° angle. A major side branch has > 2 branching levels (number of branching points before reaching a leaf) ahead, while a minor side branch has ≤ 2 branching levels ahead. The weight $w(\text{branch})$ is determined as the sum of all edge lengths, i.e. the length of the branch and all its side branches.

primary branch	longest path; starts at the root	drawn as a straight line
major side branch	> 2 branching levels ahead	deflected at 45° angle
minor side branch	≤ 2 branching levels ahead	deflected at 90° angle

Table 1: *Branch types*

In particular, the root v_0 is drawn at $(x_0 = 0,\ y_0 = 0)$ in the 2D sketch, the starting point of the neuron's primary branch. Let v_1 = child(v_0). If v_1 is no branching point, it is drawn at $(x_1 = x_0 + s,\ y_1 = 0)$, i.e. the primary branch is elongated by $s = 1$ units. If v_1 is a branching point, we compute the weight of both child branches and determine which of them is continued as a straight line and which is deflected. The same procedure is applied recursively also to side branches of the primary branch and their side branches, and so on.

As a neuron does not have a uniquely defined end point, the 2D neuron sketch ends with a fork-like terminal structure where the last major side branch and the last segment of the primary branch deflect at -45° and 45°, respectively (Figure 1B). The terminal is placed at the branching point that maximizes the weight ratio $\frac{w(\text{major\_side\_branch})}{w(\text{primary\_branch\_ahead})}$ between the major side branch that branches off at the respective point and the remaining segment of the primary branch, favouring approximately equal weights for both branches.

To minimize branch overlap, the major side branches are deflected upwards and downwards in an alternating fashion. Only in the visualized dendrograms, i.e. not affecting the measured dendrogram features, the primary branch is elongated whenever this becomes necessary to avoid side branch overlap. In such cases, the elongation factor can be annotated on the respective segment of the primary branch (Figure 1B).

2.4. Dendrogram features

Dendrogram features are computed separately for each major side branch of the neuron's primary branch. We consider the following features that can be extracted from the dendrograms:

- *branch_position*: position of the side branch along the [0,1]-normalized primary branch
- *branching_degree*: max. number of branching levels ahead
- *#major_side_branches*, *#minor_side_branches* on the side branch
- *major_side_branch_length*, *minor_side_branch_length*: average length for the respective branch type on the side branch
- *#input_synapses*, *#output_synapses* on the side branch

2.5. Synapse labels

If a vertex v_i has a synapse label, a symbol is plotted at position $(x_i,\ y_i)$ as determined during the dendrogram drawing process. There are eight classes of synapses for the AL data set: (input synapse, output synapse) x (ORN, PN, picky, broad).

For each neuron class, we employ a distinct symbol (Figure 1B): The horizontally connecting broad and picky interneurons are represented by upwards or downwards pointing triangles, respectively. The vertically projecting ORNs and PNs are represented by differently rotated squares. Input synapses are drawn in shades of blue (picky/broad) and green (ORN/PN), whereas for output synapses we employ reddish (picky/broad) or yellowish (ORN/PN) colors.

As the large number of synapses and their clustered occurrence impair readability, we sparsen the synapses, representing local clusters of synapses of the same class by a single synapse label, and distributing the labels to minimize overlap.

For synapse sparsening, all class-C synapses within a radius r (in 2D neuron coordinates) around a synapse of class C are counted. The new synapse label is placed at the centroid of all class-C synapses within the radius, and the size of the label is chosen proportional to the number of synapses that it represents: $\log(c_1 + \#\text{synapses}\ c_2)$, with c_1 determining the minimal size and c_2 a scaling factor. Synapses that have contributed to such a scaled synapse label are removed from the pool before processing the remaining synapses.

Finally, the synapse labels are distributed in the 2D plane by a greedy optimization scheme with constraints. For each synapse label, a random displacement by a small distance is evaluated with respect to whether it increases $\min(\text{dist}(l_i, l_j))$ over all synapse label pairs (l_i, l_j). The loop over all synapse labels is repeated m times, or until the minimum label distance does not increase more than a threshold value. We impose the constraint that a displacement can only be accepted if the respective synapse label remains within a radius ρ around its original location, guaranteeing that label positions are correct up to a user-specified distance ρ.

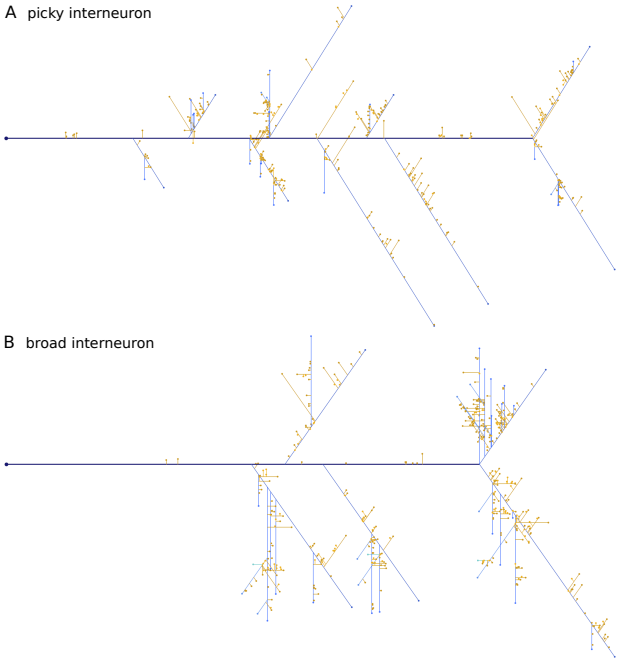

Figure 3: *Dendrogram of a picky **(A)** and a broad **(B)** interneuron (without synapses). Primary branch (thick line) and multiple levels of major side branches: shades of blue. Multiple levels of minor side branches: shades of yellow.*

3. Results and Discussion

3.1. Discriminating interneuron classes

3.1.1. Visual example

We applied our method to interneurons from the AL of the fruit fly larva (Section 2.1). The dendrograms for two archetypical representatives of the two interneuron classes (Figure 3) reveal differences in terms of the dendrogram features (Section 2.4): The picky interneuron is characterized by a larger number of major side branches occurring along the entire primary branch, whereas the broad interneuron has fewer major side branches that are clustered towards the end of the primary branch (*branch_position*). The major side branches of the picky interneuron have fewer side branches (*#major_side_branches*, *#minor_side_branches*) and lower branching degrees (*branching_degree*), whereas the major side branches of the broad interneuron have more side branches and higher branching degrees. For further examples, see Figure 1 (broad) and Figure 6 (picky).

3.1.2. Unsupervised data analysis

We computed features derived from the dendrograms (Section 2.4) for all major side branches of the picky and broad interneurons in the left AL of the fruit fly larva. Figure 4 shows the major side branches in feature space after reduction to the first two principal components of the (major side branches $\times$ features) matrix. Clearly, the major side branches of the five broad interneurons (in shades of blue) vary along the first principal component axis (PC1), whereas the major side branches of the five picky interneurons (in shades of red) vary along the second principal component axis (PC2).

Table 2 contains the coefficient contributions to the principal components ("loadings"), where high absolute values indicate a high contribution. PC1 has similar contributions from the branch number, branching degree and synapse number features. It may be regarded as a "picky to broad axis": At the extremes of PC1, we find the archetypes for the two classes "picky" (e.g. Figure 4A) and "broad" (e.g. Figure 4C). The branches of the picky neurons vary mainly along PC2 that is dominated by *branch_position* (Table 2), which renders PC2 more of a positional than a structural axis. The greater positional variation for the picky interneurons also confirms the visual impression from Figure 3.

While the major side branches of the picky and broad interneurons are well separated, outliers do exist. The broad interneurons are characterized by "heavy" side branches with a high branching degree, but they can also have a few lightweight branches that closely resemble the ones of the picky interneurons (Figure 4B, E).

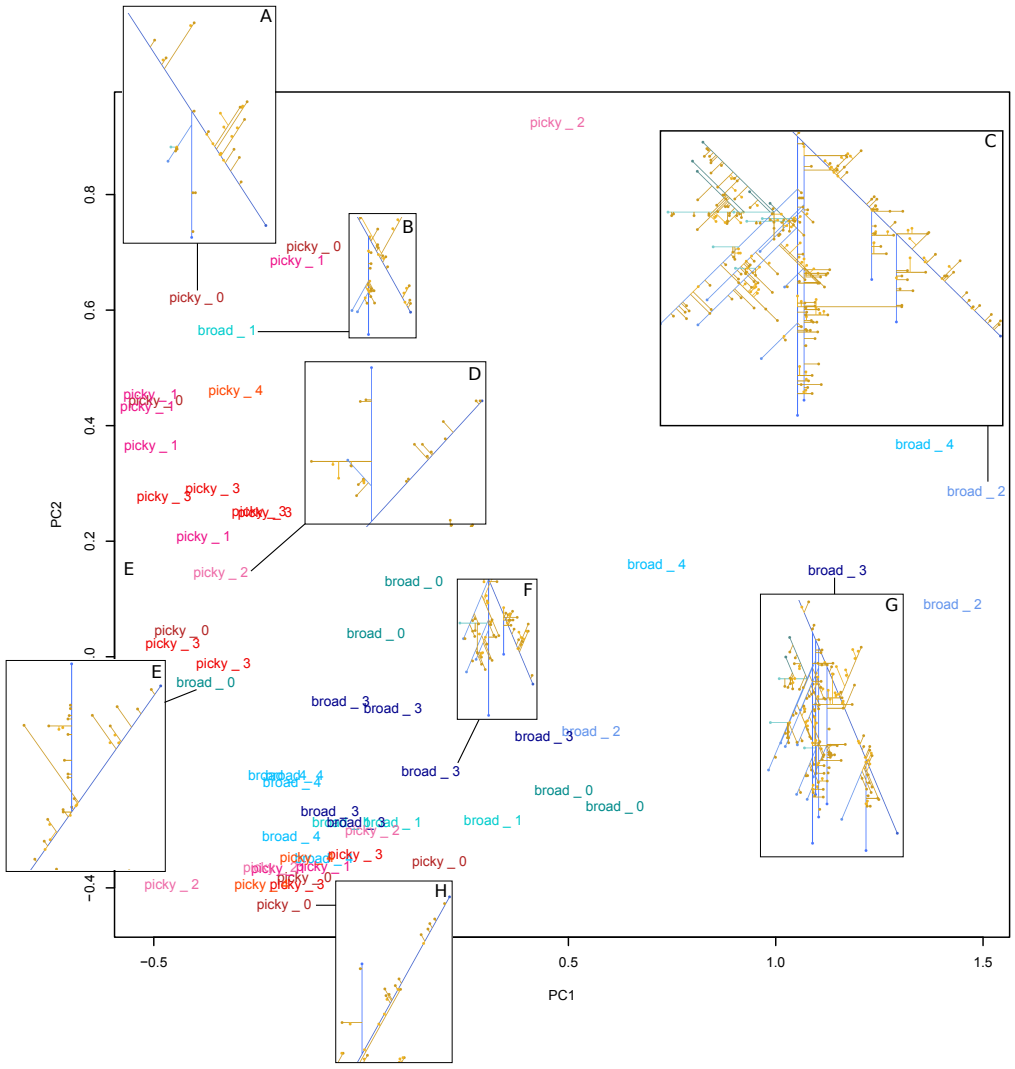

Figure 4: *PCA: Major side branches of picky (in shades of red) and broad (in shades of blue) interneurons in the space of the first two principal components that together account for 83% of the variance in the data.*

feature	PC1	PC2
major_side_branch_length	-0.09	-0.04
minor_side_branch_length	-0.11	+0.05
#major_side_branches	+0.47	+0.21
#minor_side_branches	+0.41	+0.17
branching_degree	+0.33	+0.20
#output_synapses	+0.49	-0.14
#input_synapses	+0.42	+0.19
branch_position	+0.27	-0.91

Table 2: *Loadings for the principal components in Figure 4.*

3.1.3. Classification

We also performed a classification experiment to determine whether the dendrogram features (Section 2.4) can serve to classify major side branches as belonging to a picky or to a broad interneuron. In total, there are 26 major side branches from broad interneurons and 30 from picky interneurons in the data set, i.e. the classes are roughly balanced. For classification, we employed Linear Discriminant Analysis (LDA; function *lda* from the R-package MASS) with leave-one-out cross validation.

Table 3 shows the confusion matrix for classifying the major side branches: 80% of the side branches of picky interneurons and 73% of the side branches of broad interneurons were classified correctly. Analyzing the results on a per-neuron basis (Table 4), it becomes apparent that for all picky interneurons the majority of branches were classified as "picky" and that for three out of five broad interneurons the majority of branches were classified as "broad". As noted before (cp. Section 3.1.2, Figure 4), broad neurons are characterized by especially heavy side branches, but this does not rule out the existence of smaller or lighter branches.

	True	
Predicted	broad interneuron	picky interneuron
broad interneuron	**0.73**	0.2
picky interneuron	0.27	**0.8**

Table 3: *Classification of major side branches: Confusion matrix obtained from LDA with leave-one-out cross validation.*

neuron name	**classification result**
broad_interneuron0	5 branches (2 broad, 3 picky)
broad_interneuron1	4 branches (2 broad, 2 picky)
broad_interneuron2	3 branches (3 **broad**, 0 picky)
broad_interneuron3	7 branches (7 **broad**, 0 picky)
broad_interneuron4	7 branches (5 **broad**, 2 picky)
picky_interneuron0	7 branches (1 broad, 6 **picky**)
picky_interneuron1	7 branches (2 broad, 5 **picky**)
picky_interneuron2	5 branches (1 broad, 4 **picky**)
picky_interneuron3	8 branches (1 broad, 7 **picky**)
picky_interneuron4	3 branches (1 broad, 2 **picky**)

Table 4: *LDA classification of major side branches per neuron.*

3.2. Dendrograms with synapse annotations

Synapse annotations on the reconstructed neurons are often densely clustered, such that synapse labels overlap or are completely covered by other synapse labels. Figure 5A shows a side branch of a broad interneuron with all synapses plotted at their original locations. Figure 5B demonstrates the effect of summarizing and distributing the synapse labels (Section 2.5): Labels do no longer overlap and several previously covered synapse labels become visible. Optimizing the positions of synapse annotations makes it possible to display all synapses on a neuron in one figure (Figure 1). An alternative visualization is presented in Figure 6 that provides a compact summary of the synapse content in the side branches through stacked bar charts. The size of a bar segment is proportional to the number of synapses of the respective class. Clearly, the synapse distribution at the beginning of the neuron, close to the cell body, is different from that at the end of the neuron. The first three major side branches primarily receive input via ORN synapses, whereas the last three major side branches contain synapses from all neuron classes, and these connections occur in similar numbers as input and output synapses, respectively.

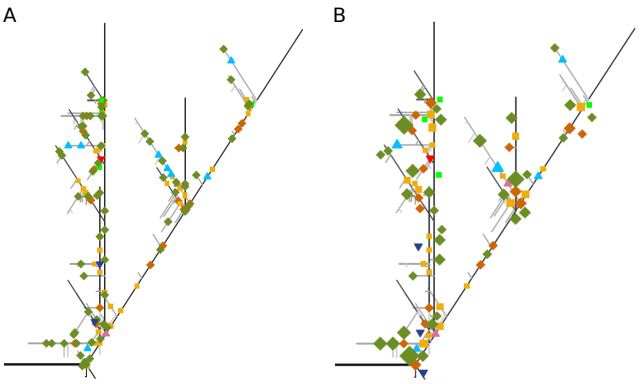

Figure 5: *Side branch of the broad interneuron from Figure 1 before **(A)** and after **(B)** summarizing and distributing synapse labels.*

3.3. Applications and limitations

3.3.1. Applications

The complex morphology of single neurons, that furthermore overlap with their neighbours, being densely packed in a compact brain circuit, prevents data analysis by visual inspection of the 3D neurons. Our collaboration partners from neurobiology are currently using the dendrogram visualizations to analyze connectivity and spatial synapse distributions for two classes of neurons from a learning and memory circuit of the larval fruit fly brain, the so-called mushroom body [ELLK*17]. The mushroom body output (MBONs) and dopaminergic (DANs) neurons are of interest as they are involved in establishing the memory for a food reward associated with an event, as well as in retrieving the memory. The dendrograms are being used both for data analysis and for presenting the results in journal figures, visualizing e.g. whether two synapse classes co-occur on the same side branch, or whether they are separated spatially, which has implications for network function.

Another application case relates to the morphological features (Section 2.4) derived from the dendrograms. Classification based on these features can be used to quantify to which extent neurons from the same developmental lineage, that have a common progenitor cell, also share morphological traits.

3.3.2. Limitations

While the static display of the whole neuron with all synapses has its merits, a disadvantage is that the level of abstraction cannot be changed. For explorative data analysis, the possibility to interactively reveal further details could be relevant, e.g. by redrawing a selected branch at higher resolution or by splitting up a synapse cluster into its members. Similarly, it could be helpful to remove detail that is hard to see, if it is not relevant for the message the figure should convey, e.g. by dropping minor side branches.

Deflecting side branches at stereoyped angles enables a compact representation, but it also leads to line crossings, especially minor side branches crossing neighbouring major side branches (see e.g. Figure 3). It remains to be evaluated whether the present version of the dendrograms or a version with more space-consuming, flattened out side branches will be perceived as more useful by researchers.

3.4. Outlook: Connectivity for a neuron ensemble

Going beyond visualizing single neurons, Figure 7 serves as an example for how the dendrograms can be utilized to analyze the function of neuron ensembles at the single synapse level. Figure 7 shows the synaptic connections between interneurons and a pair of input/ouput neurons of the AL (receptor neuron ORN 13a and projection neuron PN 13a). In the case of the broad interneuron in Figure 7A, the three involved synapse types (input from ORN, output to ORN, output to PN) always occur together in local domains

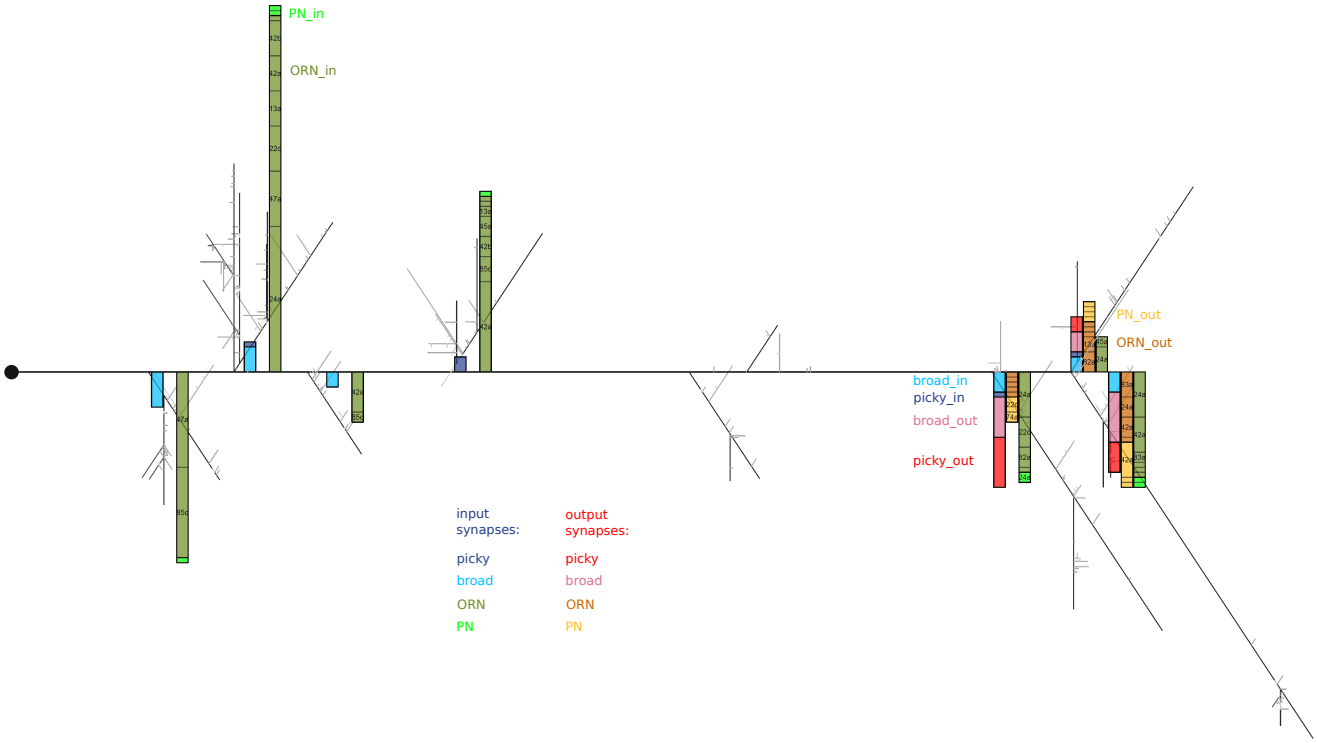

Figure 6: *Dendrogram of a picky interneuron (picky 0). The synapse distribution of each side branch is summarized by stacked bar charts.*

(zones highlighted by grey circles), whereas the picky interneuron in Figure 7B exhibits a clear spatial separation of ORN input from the two other synapse types.

The ability to display such spatial relationships is relevant in terms of analyzing neural function, as we do not only learn which neurons are connected, but also where and in which order the connections occur along the neuron, and whether signals arrive simultaneously or with a delay.

Here, the arrangement of neurons was optimized manually, while future work will be targeted at performing this automatically through penalizing structural overlap and line crossings. It is evident from Figure 7B that the interneuron connects to ORN 13a multiple times with different side branches. The interneuron contains loops that have been stretched out for the linear dendrogram representation. This linearization is a necessary abstraction as the neurons have complex morphologies and occur entangled and overlapping in a small volume, the AL, in which they form numerous connections. Visually encoding the position of a neuron's side branch in AL space on the linear dendrogram is an interesting aspect of further research.

4. Conclusions

Motivated by data sets of larval fruit fly brain circuits reconstructed from electron microscopy data, we have proposed a method to draw realistic dendrograms of 3D neuron reconstructions, that, unlike common dendrogram types, preserve branch lengths and thus cable-length distances between synapses. Supporting the visual impression that known neuron classes can be discriminated based on the dendrograms, we performed supervised and unsupervised data analysis, successfully discriminating the classes using features that describe the dendrograms.

The cable-length preserving property and the possibility to locate large numbers of synapses precisely and with minimal label overlap are the basis for an effective visualization that allows analyzing neural function also in scenarios where synapse position and temporal effects due to signal decay are relevant. The proposed dendrogram visualization is suitable for static journal figures, and it enables automated structuring and exploratory data analysis for large data sets that comprise entire brains [ZLP*18].

References

[ABS*14] AL-AWAMI A. K., BEYER J., STROBELT H., KASTHURI N., LICHTMAN J. W., PFISTER H., HADWIGER M.: NeuroLines: A subway map metaphor for visualizing nanoscale neuronal connectivity. *IEEE Trans. Vis. Comput. Graph. 20*, 12 (2014), 2369–2378. 3

[AK00] ASCOLI G. A., KRICHMAR J. L.: L-neuron: A modeling tool for the efficient generation and parsimonious description of dendritic morphology. *Neurocomputing 32-33*, Suppl.C (2000), 1003 – 1011. 3

[Asc02] ASCOLI G. A.: Neuroanatomical algorithms for dendritic modelling. *Network: Comp. in Neur. Sys. 13*, 3 (2002), 247–260. 3

[BAK*13] BEYER J., AL-AWAMI A. K., KASTHURI N., LICHTMAN J. W., PFISTER H., HADWIGER M.: ConnectomeExplorer: Query-guided visual analysis of large volumetric neuroscience data. *IEEE Trans. Vis. Comput. Graph. 19*, 12 (2013), 2868–2877. 3

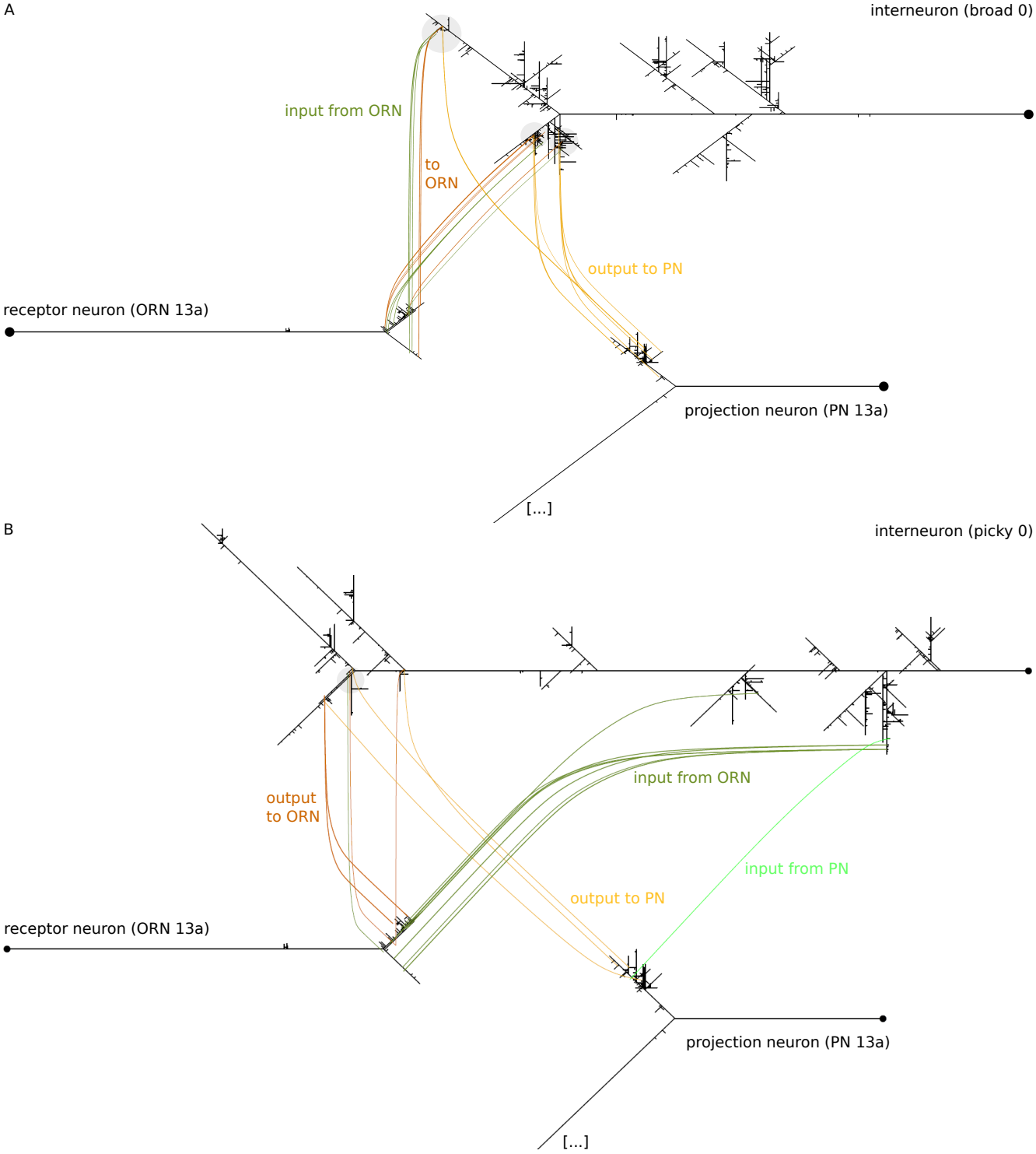

Figure 7: *Example for nanonscale connectivity in the larval fruit fly AL, an olfactory center.* ***A*** *Connectivity between a broad interneuron and receptor neuron ORN 13a, and between the interneuron and projection neuron PN 13a. Curved lines connect the synaptic sites. Filled circles highlight three contact zones where the three involved synapse types (input from receptor neuron, output to receptor neuron, output to projection neuron) occur together.* ***B*** *Connectivity between a picky interneuron and ORN/PN 13a. Here, synapses that relay input from the receptor neuron (dark green) are, with one exception (filled circle), spatially separated from the other synapse types.*

[BKC*16] BERCK M. E., KHANDELWAL A., CLAUS L., HERNANDEZ-NUNEZ L., SI G., TABONE C. J., LI F., TRUMAN J. W., FETTER R. D., LOUIS M., SAMUEL A. D., CARDONA A.: The wiring diagram of a glomerular olfactory system. *eLife 5* (may 2016), e14859. 2, 4

[BSG*09] BRUCKNER S., SOLTÉSZOVÁ V., GRÖLLER M. E., HLADUVKA J., BÜHLER K., YU J. Y., DICKSON B. J.: BrainGazer - Visual Queries for Neurobiology Research. *IEEE Trans. Vis. Comput. Graph. 15*, 6 (2009), 1497–1504. 3

[CCJdFC16] CERVANTES E. P., COMIN C. H., JR. R. M. C., DA FONTOURA COSTA L.: Data-oriented neuron classification from their parts. In *12th IEEE International Conference on e-Science, e-Science 2016, Baltimore, MD, USA, October 23-27, 2016* (2016), pp. 243–250. 3

[CdFC99] CESAR R. M., DA FONTOURA COSTA L.: Computer-vision-based extraction of neural dendrograms. *Journal of Neuroscience Methods 93*, 2 (1999), 121 – 131. 3

[CMO*16] COSTA M., MANTON J. D., OSTROVSKY A. D., PROHASKA S., JEFFERIS G. S.: NBLAST: Rapid, sensitive comparison of neuronal structure and construction of neuron family databases. *Neuron 91*, 2 (2016), 293 – 311. 3

[DEHO12] DERCKSEN V. J., EGGER R., HEGE H.-C., OBERLAENDER M.: Synaptic connectivity in anatomically realistic neural networks: Modeling and visual analysis. In *Eurographics Workshop on Visual Computing for Biology and Medicine (VCBM)* (2012), pp. 17 – 24. 3

[ELLK*17] EICHLER K., LI F., LITWIN-KUMAR A., PARK Y., ANDRADE I., SCHNEIDER-MIZELL C. M., SAUMWEBER T., HUSER A., ESCHBACH C., GERBER B., FETTER R. D., TRUMAN J. W., PRIEBE C. E., ABBOTT L. F., THUM A. S., ZLATIC M., CARDONA A.: The complete connectome of a learning and memory centre in an insect brain. *Nature 548* (Aug. 2017), 175. 2, 7

[FBO*14] FERREIRA T. A., BLACKMAN A. V., OYRER J., JAYABAL S., CHUNG A. J., WATT A. J., SJÖSTRÖM P. J., VAN MEYEL D. J.: Neuronal morphometry directly from bitmap images. *Nature Methods 11* (Sept. 2014), 982. 3

[KDS*18] KANARI L., DŁOTKO P., SCOLAMIERO M., LEVI R., SHILLCOCK J., HESS K., MARKRAM H.: A topological representation of branching neuronal morphologies. *Neuroinformatics 16*, 1 (Jan 2018), 3–13. 3

[LWA*17] LI Y., WANG D., ASCOLI G. A., MITRA P., WANG Y.: Metrics for comparing neuronal tree shapes based on persistent homology. *PLOS ONE 12*, 8 (08 2017), 1–24. 3

[RMM*16] RAJKOVIĆ K., MARIĆ D. L., MILOŠEVIĆ N. T., JEREMIC S., ARSENIJEVIĆ V. A., RAJKOVIĆ N.: Mathematical modeling of the neuron morphology using two dimensional images. *Journal of Theoretical Biology 390*, Supplement C (2016), 80 – 85. 3

[SB79] SIEGLER M. V. S., BURROWS M.: The morphology of local non-spiking interneurones in the metathoracic ganglion of the locust. *The Journal of Comparative Neurology 183*, 1 (1979), 121–147. 2

[SBS*13] SORGER J., BÜHLER K., SCHULZE F., LIU T., DICKSON B. J.: neuroMap - interactive graph-visualization of the fruit fly's neural circuit. In *IEEE Symposium on Biological Data Visualization, BioVis 2013, Atlanta, GA, USA, October 13-14, 2013* (2013), pp. 73–80. 3

[Sch11] SCHULZ H.: Treevis.net: A tree visualization reference. *IEEE Computer Graphics and Applications 31*, 6 (Nov 2011), 11–15. 3

[SCHT09] SAALFELD S., CARDONA A., HARTENSTEIN V., TOMANCAK P.: CATMAID: Collaborative Annotation Toolkit for Massive Amounts of Image Data. *Bioinformatics 25*, 15 (2009), 1984–1986. 3

[Sho53] SHOLL D.: Dendritic organization in the neurons of the visual and motor cortices of the cat. *J Anat. 87(4)* (1953), 387–406. 3

[SMB*17] SWOBODA N., MOOSBURNER J., BRUCKNER S., YU J. Y., DICKSON B. J., BÜHLER K.: Visualization and quantification for interactive analysis of neural connectivity in *Drosophila*. *Comput. Graph. Forum 36*, 1 (2017), 160–171. 3

[SMGL*16] SCHNEIDER-MIZELL C. M., GERHARD S., LONGAIR M., KAZIMIERS T., LI F., ZWART M. F., CHAMPION A., MIDGLEY F. M., FETTER R. D., SAALFELD S., CARDONA A.: Quantitative neuroanatomy for connectomics in *Drosophila*. *eLife 5* (mar 2016), e12059. 2, 3, 4

[SPA08] SCORCIONI R., POLAVARAM S., ASCOLI G. A.: L-measure: a web-accessible tool for the analysis, comparison and search of digital reconstructions of neuronal morphologies. *Nature Protocols 3* (Apr. 2008), 866–876. 3

[ZLP*18] ZHENG Z., LAURITZEN J. S., PERLMAN E., ROBINSON C. G., NICHOLS M., MILKIE D., TORRENS O., PRICE J., FISHER C. B., SHARIFI N., CALLE-SCHULER S. A., KMECOVA L., ALI I. J., KARSH B., TRAUTMAN E. T., BOGOVIC J. A., HANSLOVSKY P., JEFFERIS G. S., KAZHDAN M., KHAIRY K., SAALFELD S., FETTER R. D., BOCK D. D.: A complete electron microscopy volume of the brain of adult Drosophila melanogaster. *Cell 174*, 3 (2018), 730 – 743.e22. 8